

Flow and Heat Transfer over a Stretching Sheet Embedded In a Porous Media With Fluid-Particle Suspension

Anitha V¹, Ramakrishna Prasad² and Hanumesh Vaidya³

¹Department of Mathematics, Sir M.V.Govt. Science college, Bommanakatte-577 301, Bhadravathi, India.

²Department of Mathematics, S.V.U. Thirupati, A.P. India.

³Department of Mathematics, SSA Government First Grade College, Bellary-583 101, Karnataka, India.

ABSTRACT

A mathematical model is presented for analyzing the boundary layer flow and heat transfer of dusty fluid over a stretching sheet embedded in a porous medium. Temperature dependent fluid properties are assumed to vary as a function of the temperature. Using a similarity transformation, the governing coupled non-linear partial differential equations are transformed into a system of coupled non-linear ordinary differential equations and solved numerically by the Keller-box method. The numerical solutions are compared with the approximate analytical solutions, obtained by a perturbation technique. The analysis reveals that even in the presence of variable fluid properties the transverse velocity of the fluid is to decrease with an increase in the fluid-particle interaction parameter. This observation holds even for porous medium. Furthermore, the effects of the physical parameters on the fluid velocity, the velocity of the dust particle, the density of the dust particle, the fluid temperature, the dust-phase temperature, the skin friction, and the wall-temperature gradient are assessed through tables and graphs.

Keywords: Two-phase flow, fluid-particle interaction, variable fluid properties, stretching sheet, finite difference method.

1. INTRODUCTION

The pioneering work in the field of boundary layer flow over a continuously moving surface with a constant speed was done by Sakiadis [1-2] which has many engineering and technological applications such as extrusion process, wire and fiber coating, polymer processing, food-stuff processing, design of heat exchangers, and chemical processing equipment. Tsou et al. [3] verified the analysis of [1] experimentally and extended his work to heat transfer problem. Keeping these experimental and practical applications in view, Crane [4] extended the work of Sakiadis [1] to a stretching sheet with linear surface velocity and obtained a similarity solution to the problem. Consequently, the concept of stretching surface has drawn the attention of many researchers [5-12] to various aspects of this phenomenon, such as heat and mass transfer on horizontal/vertical plate, on inclined plates, with or without suction or blowing, steady flow, unsteady flow due to a sudden stretching of sheet or by changing the temperature of the sheet, wall temperature, magnetic field, effect of diffusion-thermo and thermal diffusion of heat and mass.

However, in addition to these above aspects, it is important to note that the porous media can be used to enhance the heat transfer rate from stretching surfaces and has numerous applications in geophysics, oil recovery techniques, heat storage systems, insulation design, grain storage, geothermal systems, heat exchangers, filtering devices, metal processing, catalytic reactors etc. Realizing these applications, Vajravelu [13] analyzed the flow and heat transfer characteristics in a saturated porous medium over an impermeable non-isothermal stretching sheet with frictional heating and internal heat generation or absorption. Further, Rees and Storesletten [14-17] presented series of papers on the effect of anisotropic permeability on free convective boundary layer flow over a vertical flat plate embedded in a porous medium and obtained interesting results for the motions induced by point sources or horizontal line sources of heat. Abel et al. [18-20] cited Ref [13] and analyzed effect of heat transfer of a non-Newtonian fluid immersed in a porous medium over a non-isothermal stretching sheet for two different cases namely prescribed surface temperature (PST), and prescribed heat flux (PHF) and concluded that fluid viscosity parameter is to decrease the wall temperature profile significantly when flow is through a porous medium. Pal and Shivakumara[21] considered the boundary layer flow in the porous medium governed by the Lapwood Forchheimer-Brinkman extended Darcy mode and studied the mixed convection from a heated vertical plate embedded in a Newtonian fluid saturated sparsely packed porous medium. Recently, Hayat et al. [22] employed Homotopy analysis method (HAM) to study Slip flow and heat transfer of a second grade fluid past a stretching sheet through a porous space.

All the above investigators restricted their analyses to the flow induced by a linear/vertical stretching sheet under different physical situations and in the absence of fluid-particle suspension. The analysis of two-phase flows in which solid spherical particles are distributed in a fluid are of interest in a wide range of technical problems such as flow through packed beds, sedimentation, environmental pollution, centrifugal separation of particles and blood rheology. The study of the boundary layer of fluid-particle suspension flow is important in determining the particle accumulation and impingement of the particle on the surface. In view of these applications, Chakrabarti [23] analyzed the boundary layer in a dusty gas. Datta and Mishra [24] investigated boundary layer flow of a dusty fluid over a semi-infinite flat plate in to two regions namely the region of high slip velocity and that of small slip velocity. Most recently, Parul and Manju [25] discussed the effect of permeability of porous medium on the motion in the fluid phase and in the dust phase by considering viscous dusty fluid between two infinitely non-conducting parallel porous plates. These researchers assumed that the thermo-physical properties of the ambient fluid particle suspension as constant. However, it is well known that (see for details Chiam [26], Hassanien [27], Subhas Abel et al. [28], and Prasad et al. [29]) these physical properties may change with temperature, especially the viscosity and the thermal conductivity. Therefore to predict the flow and heat transfer rates, it is necessary to take into account the variable fluid properties.

Motivated by these analyses, we extend the work of Vajravelu [13] by considering the temperature-dependent variable fluid properties. Thus in the present paper, we study the effects of variable thermo-physical transport properties on the fluid-particle suspension flow and heat transfer over a stretching sheet embedded in a porous media. The coupled non-linear

partial differential equations governing the problem have been transformed to a system of coupled non-linear ordinary differential equations. The transformed equations are solved numerically by a second order finite difference scheme known as the Keller-box method. Computed numerical results for the flow and heat transfer characteristics are analyzed graphs and through tables. It is expected that the results obtained will not only provide useful information for industrial application but also complement the previous works.

2. Mathematical formulation

Consider the steady flow of a viscous, and incompressible dusty fluid over a horizontal stretching sheet embedded in a porous medium with a stretching linear velocity $U_w(x) = bx$, and prescribed surface temperature $T_w(x) = A_1(x/l)$, where $b (> 0)$ and A_1 are constants (see Fig. 1 for details).

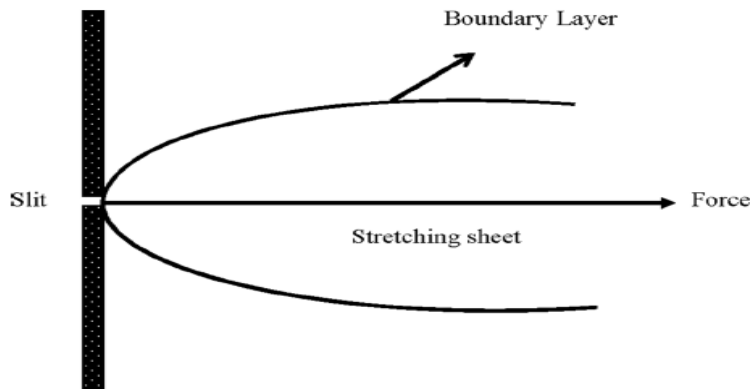


Fig. 1 Physical model and coordinate system

The thermo-physical fluid properties are assumed to be isotropic and constant, except for the fluid viscosity and the fluid thermal conductivity which are assumed to vary as a function of temperature in the following forms (see for details, Chiam [26] and Prasad et al. [29]):

$$\frac{1}{\mu} = \frac{1}{\mu_\infty} \left[1 + \gamma(T - T_\infty) \right], \quad (1)$$

$$K(T) = K_\infty \left(1 + \varepsilon \frac{T - T_\infty}{\Delta T} \right), \quad (2)$$

where μ_∞ and K_∞ are the ambient fluid viscosity and thermal conductivity respectively. ε is a small parameter known as the variable thermal conductivity parameter, T is the temperature of the fluid and $\Delta T = (T_w - T_\infty)$.

Equation (1) can be written as,

$$\frac{1}{\mu} = a(T - T_r), \quad (3)$$

where

$$a = \frac{\gamma}{\mu_\infty} \text{ and } T_r = T_\infty - \frac{1}{\gamma}. \quad (4)$$

Both a and T_r are constants and their values depend on the reference state and the thermal property of the fluid, i.e. γ (a constant). In general, $a > 0$ for liquids and $a < 0$ to gases, when $T_w > T_\infty$. The correlations between the viscosity and the temperature for air and water are given as follows:

For air: $\frac{1}{\mu} = -123.2(T - 742.6)$, based on $T_\infty = 293 \text{ K } (20^\circ\text{C})$,

and for water : $\frac{1}{\mu} = -29.83(T - 258.6)$, based on $T_\infty = 288 \text{ K } (15^\circ\text{C})$. Also, let θ_r be the

constant which is defined by

$$\theta_r = \frac{T_r - T_\infty}{\Delta T} = -\frac{1}{\gamma \Delta T}. \quad (5)$$

It is worth mentioning here that for $\gamma \rightarrow 0$ i.e. $\mu = \mu_\infty$ (constant), $\theta_r \rightarrow \infty$. It is also important to note that θ_r is negative for liquids and positive for gases. This is due to the fact that viscosity of a liquid usually decreases with increasing temperature while it increases for gases. It is assumed that the flow is generated by stretching of an elastic sheet from a slit by imposing two equal and opposite forces in such a way that sheet is intact. Under these conditions, the basic boundary-layer equations for continuity, conservation of mass (with no pressure gradient) and energy can be written as (See for details Datta and Mishra)

$$\frac{\partial u}{\partial x} + \frac{\partial v}{\partial y} = 0, \quad (6)$$

$$\rho_\infty \left(u \frac{\partial u}{\partial x} + v \frac{\partial u}{\partial y} \right) = \frac{\partial}{\partial y} \left(\mu \frac{\partial u}{\partial y} \right) - \frac{\mu(T)}{K'} u - \frac{\rho_p}{\tau} (u - u_p), \quad (7)$$

$$\left(u_p \frac{\partial u_p}{\partial x} + v_p \frac{\partial u_p}{\partial y} \right) = \frac{1}{\tau} (u - u_p), \quad (8)$$

$$\left(u_p \frac{\partial v_p}{\partial x} + v_p \frac{\partial v_p}{\partial y} \right) = \frac{1}{\tau} (v - v_p), \quad (9)$$

$$\frac{\partial}{\partial x} (\rho_p u_p) + \frac{\partial}{\partial y} (\rho_p v_p) = 0, \quad (10)$$

$$u \frac{\partial T}{\partial x} + v \frac{\partial T}{\partial y} = \frac{\partial}{\partial y} \left(\alpha(T) \frac{\partial T}{\partial y} \right) + \frac{\rho_p c_s}{\gamma_T \rho_\infty c_p} (T_p - T), \quad (11)$$

$$u_p \frac{\partial T_p}{\partial x} + v_p \frac{\partial T_p}{\partial y} = -\frac{1}{\gamma_T} (T_p - T), \quad (12)$$

where (u, v) and (u_p, v_p) are the velocities components of the fluid and particle phases along the x and y axes respectively. Furthermore μ and ρ_∞ are the coefficients of viscosity of the fluid and the density of the fluid. Here $\tau = 1/k$ is the relaxation time of particles, $k = 6\pi\mu_\infty D$ is the Stokes' constant, and D is the average radius of the dust particles. Further, σ is the electrical conductivity, K' permeability of the porous medium, and ρ_p is the mass of the dust particles per unit volume of the fluid: T and T_p are respectively the temperatures of

the fluid and the dust particles. Further, c_p and c_s are respectively the specific heat capacity of the fluid and specific heat capacity of the dust particles, γ_T is the temperature relaxation time ($= 3Pr \gamma_p c_s / 2c_p$), γ_p is the velocity relaxation time ($= 1/k$), and Pr is the usual Prandtl number.

The last term in equation (7) represents the force due to the relative motion between the fluid and the dust particles. In such a case the force between dust and fluid is proportional to the relative velocity. $\alpha(T) = K(T) / \rho_\infty c_p$ is the thermal diffusivity of the fluid: It varies as a linear function of temperature. In deriving these equations the Stokesian drag force is considered for the interaction between the fluid and the particle phases. The appropriate boundary condition on velocity and temperature are :

$$u = U_w(x) = bx, \quad v = 0, \quad T = T_w = A_1(x/l) \quad \text{at} \quad y = 0, \quad (13)$$

$$u \rightarrow 0, \quad u_p \rightarrow 0, \quad v_p \rightarrow v, \quad \rho_p \rightarrow k\rho_\infty, \quad T \rightarrow T_\infty, \quad T_p \rightarrow T_\infty \quad \text{as} \quad y \rightarrow \infty.$$

Here b is a constant known as stretching rate, A_1 is a constant and l is the characteristic length. Now, let the dimensionless similarity variable be

$$\eta = \sqrt{\frac{b}{v_\infty}} y \quad (14)$$

and the dimensionless similarity functions are

$$u = bx f'(\eta), \quad v = -\sqrt{bv_\infty} f(\eta), \quad u_p = bx F(\eta), \quad v_p = \sqrt{bv_\infty} G(\eta). \quad (15)$$

$$\rho_r = H(\eta), \quad T - T_\infty = (T_w - T_\infty) \theta(\eta), \quad T_p - T_\infty = (T_w - T_\infty) \theta_p(\eta), \quad (T_w - T_\infty) = A(x/l).$$

Substituting the expressions for variable fluid viscosity and the variable fluid thermal conductivity from the equations (1) and (2) into equations (6) to (13) and making use of similarity equations from (14)-(15), we obtain

$$\left(\frac{f''}{(1-\theta/\theta_r)} \right)' + f f'' - f'^2 - \frac{K_1}{(1-\theta/\theta_r)} f' + \beta H(F - f') = 0,$$

$$GF' + F^2 + \beta(F - f') = 0$$

$$GG' + \beta(f + G) = 0$$

$$GH' + HG' + FH = 0 \quad (16)$$

$$((1 + \varepsilon\theta)\theta')' + Pr(f\theta' - f'\theta) + \frac{2}{3}\beta H(\theta_p - \theta) = 0$$

$$2F\theta_p + G\theta_p' + L_0\beta(\theta_p - \theta) = 0$$

and

$$f' = 1, \quad f = 0, \quad \theta = 1 \quad \text{at} \quad y = 0, \quad (17)$$

$$f' \rightarrow 0, \quad F \rightarrow 0, \quad G \rightarrow -f, \quad H \rightarrow k, \quad \theta \rightarrow 0, \quad \theta_p \rightarrow 0 \quad \text{as} \quad y \rightarrow \infty.$$

where a prime denotes differentiation with respect to η . Here $\rho_r = \rho_p / \rho_\infty$ is the relative density, $K_1 = \gamma_\infty / K'b$ is the permeability or porous parameter, $\beta = 1/b\tau$ is the fluid particle interaction parameter, $\theta_r = 1/\gamma(\Delta T)$ is the fluid viscosity parameter, which is negative for liquids and positive for gases, $Pr = v_\infty / \alpha_\infty$ is the Prandtl number, and ε is a small

parameter known as the variable thermal conductivity parameter and $L_0 = \tau/\gamma_T$ is the temperature relaxation parameter. The value of θ_r is determined by the viscosity of the fluid under consideration and the operating temperature difference. If θ_r is large, in other words, if $(T_\infty - T_w)$ is small, the effects of variable viscosity on the flow can be neglected. On other hand, for smaller values of θ_r , either the fluid viscosity changes markedly with temperature or the operating temperature difference is high. In either case, the effect of the variable fluid viscosity is expected to be very important. Also let us keep in mind that the liquid viscosity varies differently with temperature compared to the gas viscosity. Therefore it is important to note that θ_r is negative for liquids and positive for gases.

3. SOLUTIONS FOR SOME SPECIAL CASES

In the limiting case of $\theta_r \rightarrow \infty$ and $\varepsilon = 0, K_1 = 0$, with magnetic field the system of equations (16) reduces to those of Vajravelu and Nayfeh [32]. Further, when the variable thermo-physical properties, fluid particle interaction and the permeability parameter are absent, equations are similar to the ones studied by Crane [4], and Grubka and Bobba [6]. In the absence of variable fluid properties, the boundary layer flow and heat transfer problem degenerates. In this case, the approximate analytical solutions for the velocity field and temperature fields are obtained via perturbation analysis. These solutions are useful and serve as a baseline for comparison with the solutions obtained via numerical schemes.

4. ANALYTICAL SOLUTION BY PERTURBATION

For small β , that is for low particle interaction, let us perturb the flow and heat transfer fields as

$$\begin{aligned}
 f &= f_0 + \beta f_1 + O(\beta^2), \\
 F &= F_0 + \beta F_1 + O(\beta^2), \\
 G &= G_0 + \beta G_1 + O(\beta^2), \\
 H &= H_0 + \beta H_1 + O(\beta^2), \\
 \theta &= \theta_0 + \beta \theta_1 + O(\beta^2), \\
 \theta &= \theta_{p0} + \beta \theta_{p1} + O(\beta^2),
 \end{aligned}
 \tag{18}$$

where the perturbations are small compared with the mean or the zeroth-order quantities. With the help of (18) equations (16) and the boundary conditions (17) become

$$\begin{aligned}
 f_0''' + f_0 f_0'' - (f_0')^2 - K_1 f_0' &= 0, \\
 G_0 F_0' + F_0^2 &= 0, \\
 G_0 G_0' &= 0, \\
 G_0 H_0' + H_0 G_0' + F_0 H_0 &= 0, \\
 \theta_0'' + \text{Pr} (f_0 \theta_0' - f_0' \theta_0) &= 0, \\
 2F_0 \theta_{p0} + G_0 \theta_{p0}' &= 0,
 \end{aligned} \tag{19}$$

$$\begin{aligned}
 f_0' = 1, \quad f_0 = 0, \quad \theta_0 = 1 \quad y = 0, \\
 f_0' \rightarrow 0, \quad F_0 \rightarrow 0, \quad G_0 \rightarrow -f_0, \quad H_0 \rightarrow k, \quad \theta_0 \rightarrow 0, \quad \theta_{p0} \rightarrow 0 \quad \text{as } y \rightarrow \infty,
 \end{aligned}$$

to the zeroth-order, and

$$\begin{aligned}
 \theta_1'' + \text{Pr} (f_0 \theta_1' - f_0' \theta_1) &= \frac{2}{3} H_0 (\theta_{p0} - \theta_0) - \text{Pr} (f_1 \theta_0' - f_1' \theta_0), \\
 G_0 \theta_{p1}' + 2F_0 \theta_{p1} &= -2F_1 \theta_{p0} - G_1 \theta_{p0}' + L_0 (\theta_0 - \theta_{p0}),
 \end{aligned} \tag{20}$$

$$\begin{aligned}
 f_1' = 0, \quad f_1 = 0, \quad \theta_1 = 0 \quad y = 0, \\
 f_1' \rightarrow 0, \quad F_1 \rightarrow 0, \quad G_1 \rightarrow -f_1, \quad H_1 \rightarrow k, \quad \theta_1 \rightarrow 0, \quad \theta_{p1} \rightarrow 0 \quad \text{as } y \rightarrow \infty,
 \end{aligned}$$

to the first-order. The exact solutions for the zeroth-order velocity components f_0, G_0, F_0 , particle density H_0 and temperature θ_0 satisfying the boundary conditions are

$$\begin{aligned}
 f_0 = A_2 + B_2 \exp(-\alpha\eta), \quad F_0 = 0, \quad G_0 = -A_2, \quad H_0 = k, \\
 \theta_0(\eta) = \exp\left(-\frac{\text{Pr}}{\alpha}\eta\right) \frac{M\left(\frac{\text{Pr}}{\alpha^2}-1, 1+\frac{\text{Pr}}{\alpha^2}, -\frac{\text{Pr}}{\alpha^2}e^{-\alpha\eta}\right)}{M\left(\frac{\text{Pr}}{\alpha^2}-1, 1+\frac{\text{Pr}}{\alpha^2}, -\frac{\text{Pr}}{\alpha^2}\right)}, \quad \theta_{p0}(\eta) = 0
 \end{aligned} \tag{21}$$

where $A_2 = 1/\alpha$, $B_2 = -1/\alpha$, $\alpha = \sqrt{1+K_1}$.

Similarly the exact solutions for the first-order velocity components, first-order particle density and temperature, satisfying the differential equations and the boundary conditions are

$$\begin{aligned}
 f_1 = \left\{-kB_2/(A_2\alpha - B_2\alpha + 2Mn)\right\} e^{-\alpha\eta} + \alpha\eta e^{-\alpha\eta} - 1, \quad F_1 = -(B_2/A_2)e^{-\alpha\eta}, \\
 G_1 = -(B_2/A_2)e^{-\alpha\eta} - \left\{-kB_2/(A_2\alpha - B_2\alpha + 2K_1)\right\}, \quad H_1 = 0, \quad \theta_{p1} = -\frac{2}{3\text{Pr}G_0} \int_{\eta}^{\infty} \theta_{p0}(z) dz.
 \end{aligned} \tag{22}$$

The solution θ_1 may be obtained by solving the inhomogeneous equation it satisfies, using the standard variation of constant method. The results of the present work, in the absence of β , are compared with the available results in the literature, and are shown in tables 1 and 2. The results in tables 1 and 2 reveal very good agreement between the numerical results and the results available in the literature.

The physical quantities of interest here in the study are, the skin friction coefficient c_f and the Nusselt number Nu : They are defined by

$$c_{fx} = \frac{2\tau_w(x)}{\rho u_w^2}, \quad Nu_x = \frac{q_w x}{k_\infty (T_w - T_\infty)}, \quad (23)$$

where $\tau_w(x) = -\mu_w \left(\frac{\partial u}{\partial y} \right)_{at\ y=0}$ and $q_w(x) = -k_\infty \left(\frac{\partial T}{\partial y} \right)_{at\ y=0}$.

5. NUMERICAL PROCEDURE

The system of equations (16) is coupled and highly non-linear. Exact analytical solutions are not possible for the complete set of equations and therefore we use the efficient numerical method with second order finite difference scheme known as the Keller-Box method (For details see Cebeci and Bradshaw [30], Keller [31], and Vajravelu and Prasad [32]). The coupled boundary value problem (16,17); third order in $f(\eta)$, first order in $F(\eta), G(\eta), H(\eta), \theta_p(\eta)$ and second order in $\theta(\eta)$, respectively; is reduced to a system of nine simultaneous ordinary differential equations of first order with nine unknowns, by assuming $f = f_1, f' = f_2, f'' = f_3, \theta = \theta_1, \theta' = \theta_2$. To solve this system of equations we require nine initial conditions whilst we have only two initial conditions $f(0), f'(0)$ on $f(\eta)$ and one initial condition $\theta(0)$ on $\theta(\eta)$. The other six initial conditions $f''(0), F(0), G(0), H(0), \theta'(0)$ and $\theta_p(0)$ are not prescribed: However, the values of $f'(\eta), F(\eta), G(\eta), H(\eta), \theta(\eta)$ and $\theta_p(\eta)$ are known as $\eta \rightarrow \infty$. Now, we employ the Keller-Box scheme where these six boundary conditions are utilized to produce six unknown initial conditions at $\eta = 0$. To select η_∞ , we begin with some initial guess values and solve the boundary value problem with some particular set of parameters to obtain $f''(0), F(0), G(0), H(0), \theta'(0)$ and $\theta_p(0)$. Thus, we start with the initial approximations as $f''(0) = \delta_1, F(0) = \delta_2, G(0) = \delta_3, H(0) = \delta_4$, and $\theta_p(0) = \delta_6$.

Let δ_i^* ($i = 1, 2, 3, 4, 5, 6$) be the correct values of $f''(0), F(0), G(0), H(0), \theta'(0)$ and $\theta_p(0)$. We integrate the resulting system of nine ordinary differential equations using fourth order Runge-Kutta method and obtain the values of $f''(0), F(0), G(0), H(0), \theta'(0)$ and $\theta_p(0)$. The solution process is repeated with another larger value of η_∞ until two successive values of $f''(0), F(0), G(0), H(0), \theta'(0)$ and $\theta_p(0)$ differ only after desired digit signifying the limit of the boundary along η . The last value of η_∞ is chosen as appropriate value for that particular set of parameters. Finally, the problem can be solved numerically using a second order finite difference scheme known as the Keller-Box method. The numerical solutions are obtained in four steps as follows:

- Reduce the systems of equations (16) and (17) to a system of first-order equations;
- Write the difference equations using central differences;

- Linearize the algebraic equations by Newton’s method, and write them in matrix-vector form; and
- Solve the linear system by the block tri-diagonal elimination technique.

For the sake of brevity, the details of the numerical procedure are not presented here. It is also important to note that the computational time for each set of input parameters should be sort. Because physical domain in this problem is unbounded, whereas the computational domain has to be finite, we apply the far field boundary conditions for the similarity variable η at finite value denoted by η_{\max} . We ran our bulk of computations with the value $\eta_{\max} = 7$, which is sufficient to achieve the far field boundary conditions asymptotically for all values of the parameters considered. For numerical calculations, a uniform step size of $\Delta\eta = 0.01$ is found to be satisfactory and the solutions are obtained with an error tolerance of 10^{-6} in all the cases. To assess the accuracy of the present method, comparison of the skin friction $f''(0)$ and the wall-temperature gradient $\theta'(0)$ between the present results and previously published results are made, for several special cases in which the fluid-particle interaction parameter and thermo-physical fluid properties are neglected (see Table 1). It was found from Tables 1 and 2 that the present results agree very well with those of analytical solutions given by Grubka and Bobba [6], Andersson et al. [7], Ali [8] and Chen [9].

6. RESULTS AND DISCUSSION

In this section, we analyze the effects of the pertinent parameters, namely, the fluid-particle interaction parameter β , permeability or porous parameter K_1 , the variable fluid viscosity parameter θ_r , the variable thermal conductivity parameter \mathcal{E} , and the Prandtl number Pr on the flow and heat transfer of fluid-particle suspension over a horizontal stretching sheet. Approximate analytical solutions are obtained via perturbation method for the special case (when $\theta_r \rightarrow \infty$, $K_1 = 0$ and $\mathcal{E} = 0$). Temperature relaxation parameter L_0 is chosen as unity throughout the computations. In order to get a clear insight into the physical problem, we present the numerical results graphically in Figs. 2-7. These figures depict respectively the velocity profiles (f, f') ; the particle-suspension velocity profiles (F, G) ; and the temperature of the fluid and the dust phase profiles (θ, θ_p) . The computed numerical results are recorded in table 3 to show the behavior of the skin friction; the particle velocity and the density components; the temperature gradient and the dust-phase temperature at the sheet for different values of the governing parameters.

The transverse velocity f , the horizontal velocity f' , and the particle transverse velocity and horizontal velocity $(F(\eta), G(\eta))$ profiles are shown graphically in Figs. 2(a)-2(d) for different values of K_1 and β . The general trend is that f' , F and G decrease monotonically, whereas f increases as the distance increases from stretching sheet. It is observed from these figures that the horizontal velocity and transverse velocity profiles decrease with an increase in the permeability parameter. As a consequence, the magnitude Darcian body forces decreases (which is inversely proportional to the permeability). The Darcian resistance acts to decelerate the fluid particles in continua. This resistance diminishes as permeability of the medium increases. So gradually less drag is experienced by the flow and flow retardation is thereby decreased. This observation holds true even with particle

velocity component $F(\eta)$, but quite opposite is true with $G(\eta)$. It is noticed that the effect of increasing values of fluid-particle interaction parameter β is to reduce the fluid velocity in the boundary layer and increase the dust phase transverse velocity, as well as the horizontal velocity $F(\eta)$.

Figs. 3(a) and 3(b) exhibit the velocity profiles for several sets of values of the fluid viscosity parameter θ_r , and the fluid-particle interaction parameter β . From the graphical representation we infer that the effect of increasing values of the fluid viscosity parameter θ_r , is to decrease the momentum boundary layer thickness. Also, as θ_r , approaches zero the boundary layer thickness decreases and the horizontal velocity distribution tends to zero [see Fig. 3(b)] asymptotically. This is due to the fact that for a given fluid (air or water), when \mathcal{D} is fixed, smaller θ_r , implies higher temperature difference between the wall and the ambient fluid. The results presented here demonstrate clearly that θ_r , the indicator of the variation of fluid viscosity with temperature, has a substantial effect on the horizontal velocity components f' , as well as the transverse velocity f and hence on the skin friction. This phenomenon is true with zero and non-zero values of the fluid-particle interaction parameter β .

In Figs. 4–7, the numerical results for the fluid temperature and the dust-phase temperature $(\theta(\eta), \theta_p(\eta))$ are presented for several sets of values of the governing parameters. The general trend is that the fluid-temperature distribution is unity at the wall; whereas the dust-phase temperature is not. However, with the changes in the governing parameters both asymptotically tend to zero as the distance increases from the boundary. Fig. 4 illustrates the effect of the permeability parameter and the fluid-interaction parameter on $\theta(\eta)$. The effect of increasing values of the permeability parameter K_I is to increase the fluid temperature $\theta(\eta)$ and also the dust-phase temperature $\theta_p(\eta)$. Hence, there is an increase in the temperature profile $\theta(\eta)$ as well as the dust-phase profile. The effect of fluid interaction parameter is to decrease the temperature profile which in turn reduces the thermal boundary layer thickness; whereas it enhances the dust phase temperature at the wall and hence increases the thickness of the dust phase temperature.

Figs. 5(a) and 5(b) exhibit the fluid-temperature distribution and dust-phase temperature distribution for several sets of values of the variable viscosity parameter θ_r , and the fluid-particle interaction parameter. From the graphical representation, we observe that the effect of increasing values of the variable viscosity parameter θ_r is to enhance both the fluid-temperature as well as the dust-phase temperature. This is due to the fact that an increase in the variable viscosity parameter θ_r results in an increase in the thermal boundary layer thickness. This is very much noticeable for zero values of fluid-particle interaction parameter as compared to the larger values. The graphs for the fluid-temperature profile $\theta(\eta)$ and dust-phase temperature $\theta_p(\eta)$ for different values of the variable thermal conductivity parameter \mathcal{E} are respectively shown in Figs. 6(a) and 6(b). These figures demonstrate that an increase in the value of thermal conductivity parameter \mathcal{E} results in increasing the temperature profile $\theta(\eta)$. This is due to the fact that the assumption of temperature-dependent thermal

conductivity (linear form) implies a reduction in the magnitude of the transverse velocity by a quantity $\partial K(T)/\partial y$ as can be seen from heat transfer equation.

Figs. 7(a) and 7(b) are drawn to display the fluid-temperature profile $\theta(\eta)$ and dust-phase temperature $\theta_p(\eta)$ for different values of the Prandtl number in the absence of the fluid-interaction parameter, respectively. We observe that the effect of increasing values of the Prandtl number Pr is to decrease both $\theta(\eta)$ as well as $\theta_p(\eta)$. Physically it means that an increase in the Prandtl number means a decrease in the thermal conductivity K_∞ : Hence, there is a decrease in the thermal boundary layer thickness. This behavior can be seen even in the presence of fluid interaction parameter.

Finally, the effects of all the physical parameters on the surface-velocity gradient, the particle-velocity components, particle-density component, the temperature gradient and the dust-phase temperature, respectively, at the sheet are depicted in Table 3. It is of interest to note that the effect of increasing values of the variable viscosity parameter, the porous parameter and the fluid-particle interaction parameter is to increase the magnitude of the skin friction coefficient. The effects of the variable thermal conductivity parameter, the variable viscosity parameter and the porous parameter are to decrease the magnitude of the temperature gradient at the sheet; whereas reverse trend is observed with an increase in the Prandtl number as well as the fluid interaction parameter. From Table 3, it is further noticed that the effect of fluid interaction parameter is to increase the dust-phase temperature as well as the particle transverse velocity component $F(0)$. This observation is true for zero and non-zero values of the porous parameter.

7. CONCLUSION

Some of the interesting findings of the study are summarized below.

- In the presence of temperature-dependent thermo-physical properties, the effect of increasing values of the fluid interaction parameter and the permeability parameter is to decrease the velocity throughout the boundary layer. However, quite the opposite is true with dust phase velocity profiles.
- The effect of increasing values of fluid viscosity parameter is to decrease the velocity boundary layer thickness. However, it enhances the thermal boundary layer thickness. This phenomenon is true even with the fluid-particle suspension parameter.
- The effect of variable thermal conductivity parameter is to enhance the fluid temperature as well as the particle phase temperature in the flow region.
- The thermal boundary layers of the fluid and the dust phase are highly influenced by the Prandtl number. The effect of Pr is to decrease the thermal boundary layer thickness.
- Of all the parameters, the variable thermo-physical fluid property parameters have strong effects on the drag, heat transfer characteristics, the horizontal velocity and the temperature fields.

TABLES:

Table 1. Comparison of skin friction for different values of the Porous parameter when $\beta_r = \varepsilon = 0.0$ and $\theta_r \rightarrow \infty$.

K_1	Present results	Andersson et al. [7]	Exact Solution
0.0	-1.0001	-1.0000	-1.0000
0.5	-1.2249	-1.2247	-1.2247
1.0	-1.414	-1.414	-1.414
1.5	-1.581	-1.581	-1.582
2.0	-1.73205	-1.73350	-1.73205

Table 2. Comparison of wall-temperature gradient $\theta'(0)$ for different values of the Prandtl Number for constant surface temperature when $\theta_r \rightarrow \infty$, $\varepsilon = 0.0$, $\beta = 0$ and $K_1 = 0.0$.

Pr	Present results	Grubka and Bobba [7]	Ali [8]	Chen [9]
0.01	-0.01017936	-0.0099		-0.0091
0.72	-0.4631462	-0.4631	-0.4617	-0.46315
1.0	-0.5826707	-0.5820	-0.5801	-0.58199
3.0	-1.16517091	-1.1652	-1.1599	-1.16523
5.0	-1.56800866	-----	-----	-----
10.0	-2.308029	-2.3080	-2.2960	-2.30796
100.0	-7.769667	-----	-----	-----

Table 3: Values of the skin friction, the particle velocity components, the particle density component, the temperature gradient and the temperature of the dust particle at the wall for different values of the physical parameters.

Pr	ε	θ_r	K_1	β	$f''(0)$	$F(0)$	$G(0)$	$H(0)$	$\theta'(0)$	$\theta_p(0)$
1.0	0.0	0.0	0.0	0.0	-1.00015	0.00000	-0.97382	0.20000	-1.000140	0.00000
				1.0	-1.05395	0.52159	-0.32762	0.26572	-1.21223	0.39785
				2.0	-1.07784	0.70818	-0.07737	0.52056	-1.290571	0.60459
				3.0	-1.09489	0.78917	-0.00661	1.67711	-1.331141	0.71187
			0.5	0.0	-1.22498	0.00000	-0.81064	0.20000	-0.94656	0.00000
				1.0	-1.26851	0.52146	-0.27277	0.26609	-1.162988	0.43138
				2.0	-1.28854	0.70817	-0.06468	0.52052	-1.239744	0.61700
				3.0	-1.30292	0.78909	-0.00577	1.59296	-1.28042	0.71317
			1.0	0.0	-1.41432	0.00000	-0.70535	0.20000	-0.90194	0.00000
				1.0	-1.45223	0.52145	-0.23825	0.26615	-1.121731	0.45608
				2.0	-1.46979	0.70817	-0.05667	0.52003	-1.196771	0.62525
				3.0	-1.48246	0.78901	-0.00524	1.52775	-1.237092	0.71404
			2.0	0.0	-1.73215	0.00000	-0.57708	0.20000	-0.832988	0.00000
				1.0	-1.76326	0.52145	-0.19616	0.26614	-1.0.5494	0.49087
				2.0	-1.77779	0.70816	-0.04686	0.51900	-1.12634	0.63584

1.0	0.1	-10.0	0.5	3.0	-1.78831	0.78889	-0.00459	1.43136	-1.165365	0.71518	
				0.0	-1.21744	0.00000	-0.78636	0.20000	-0.869809	0.00000	
				1.0	-1.34587	0.52082	-0.26190	0.26700	-1.073854	0.44564	
				2.0	-1.36781	0.70797	-0.06166	0.52328	-1.144771	0.62294	
		-5.0	0.5	3.0	-1.38334	0.78904	-0.00554	1.57683	-1.182618	0.71392	
				0.0	-1.36441	0.00000	-0.76382	0.20000	-0.858874	0.00000	
				1.0	-1.41778	0.52031	-0.25211	0.26777	-1.06338	0.45230	
				2.0	-1.44157	0.70782	-0.05901	0.52549	-1.133600	0.62550	
		-1.5	0.5	3.0	-1.45818	0.78900	-0.00535	1.56064	-1.171181	0.71421	
				0.0	-1.63335	0.00000	-0.87817	0.20000	-0.815650	0.00000	
				1.0	-1.72756	0.51875	-0.21609	0.27031	-1.019397	0.47868	
				2.0	-1.76318	0.70734	-0.04960	-0.53236	-1.086136	0.63481	
1.0	0.0	-5.0	0.5	3.0	-1.78529	0.78883	-0.00468	1.48823	-1.12225	0.71528	
				0.0	-1.36578	0.00000	-0.76469	0.20000	-0.923053	0.00000	
				1.0	-1.41926	0.52026	-0.25230	0.26781	-1.140651	0.44507	
				2.0	-1.44310	0.70780	-0.05903	0.52570	-1.215927	0.62262	
		0.2	-5.0	0.5	0.0	-1.36317	0.00000	-0.76301	0.20000	-0.804383	0.00000
					1.0	-1.41644	0.52036	-0.25194	0.26772	-0.997784	0.45899
					2.0	-1.44017	0.70784	-0.059	0.52530	-1.063699	0.62805
					0.0	-1.36101	0.00000	-0.76157	0.20000	-0.716511	0.00000
		0.4	-5.0	0.5	1.0	-1.41407	0.52044	-0.25167	0.26763	-0.891964	0.47102
					2.0	-1.43770	0.70787	-0.05899	0.52494	-0.950924	0.63236
					0.0	-1.35983	0.00000	-0.76055	0.20000	-0.69308	0.00000
					1.0	-1.41330	0.52047	-0.25164	0.26757	-0.88966	0.55769
0.72	0.1	-5.0	0.5	2.0	-1.43667	0.70788	-0.05901	0.52473	-0.942570	0.70601	

FIGURES:

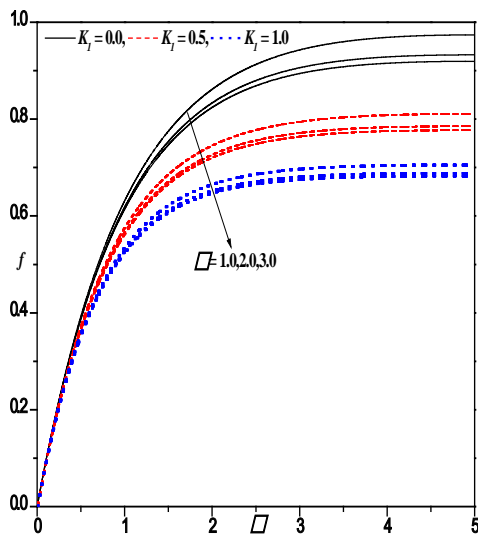


Fig.2(a): Variation of Transverse velocity profiles for different values of λ and K_i , with $\lambda = 0.0, K_i = 0.0, Pr = 1.0$.

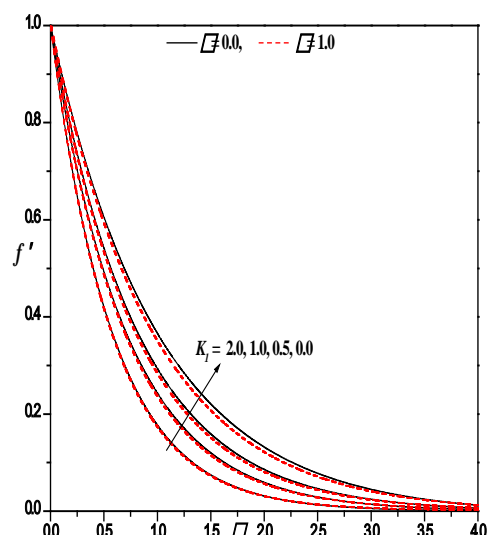


Fig.2(b): Horizontal velocity profiles for different values of λ and K_i , with $\lambda = 0.0, K_i = 0.0, Pr = 1.0$.

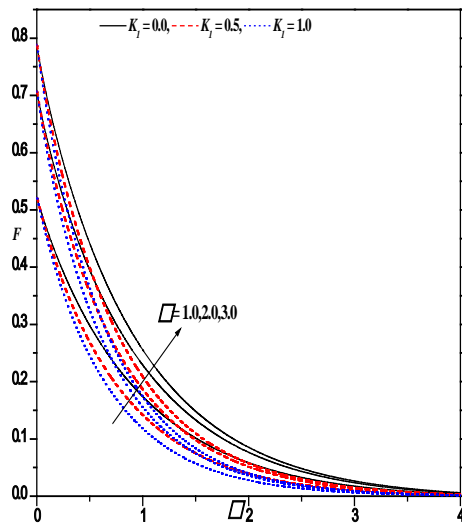


Fig 2(c) : Variation of particle velocity components for different values of α and K_1 with $\beta = 0.0, \gamma = 0.0, Pr = 1.0$.

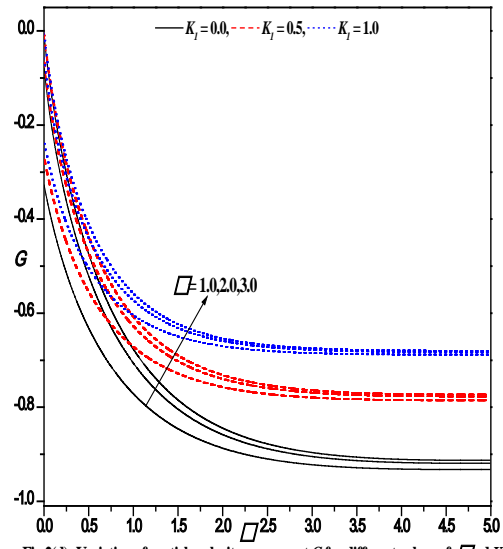


Fig 2(d) : Variation of particle velocity component G for different values of α and K_1 with $\beta = 0.0, \gamma = 0.0, Pr = 1.0$.

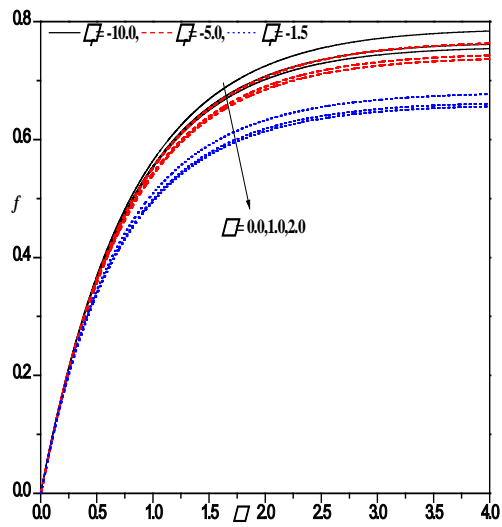


Fig 3(a) : Variation of fluid transverse velocity profiles for different values of α and β with $K_1 = 0.5, \gamma = 0.1, Pr = 1.0$.

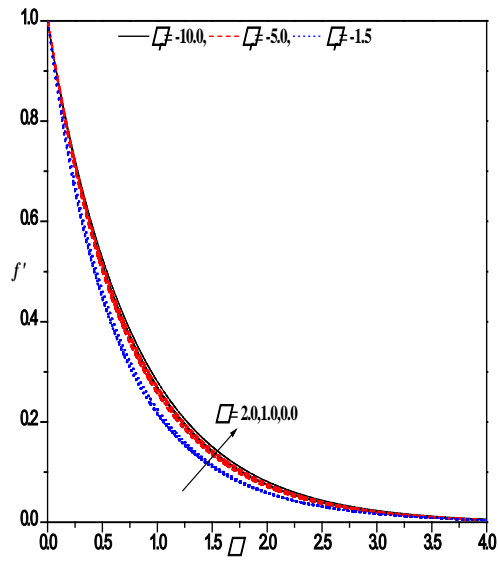


Fig 3(b) : Variation of fluid velocity profiles for different values of α and β with $K_1 = 0.5, \gamma = 0.1, Pr = 1.0$.

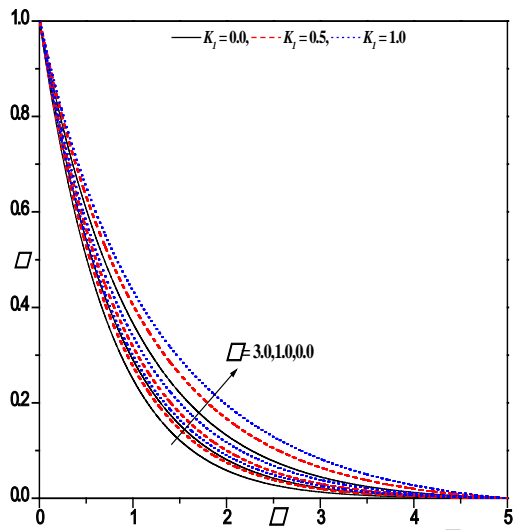


Fig.4(a): Variation of Temperature profiles for different values of K_1 and K_2 , with $K_3 = 0.0, K_4 = 0.0, Pr = 1.0$.

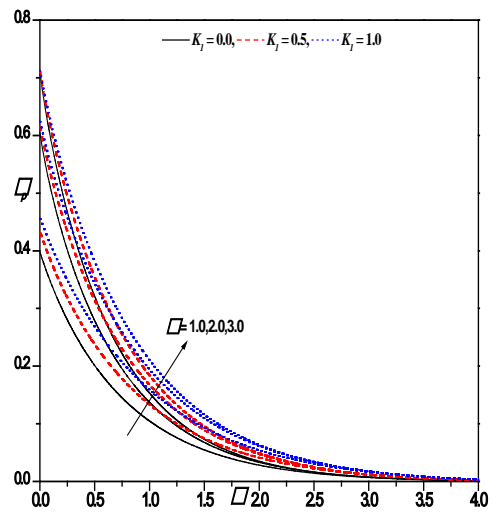


Fig.4(b): Variation of dust phase Temperature profiles for different values of K_1 and K_2 , with $K_3 = 0.0, K_4 = 0.0, Pr = 1.0$.

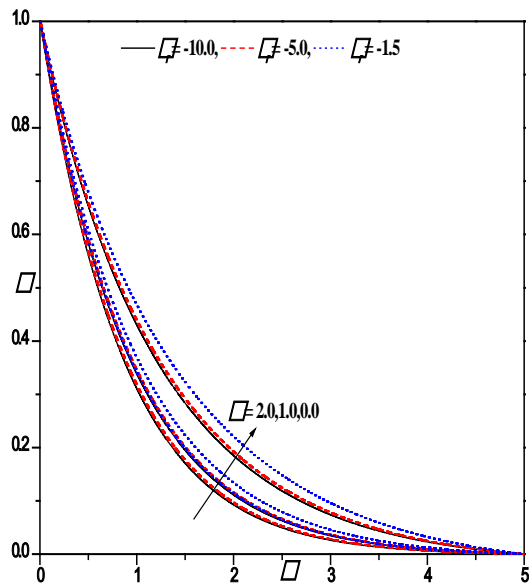


Fig. 5(a) : Temperature profiles for different values of K_1 and K_2 with $K_3 = 0.5, K_4 = 0.1, Pr = 1.0$.

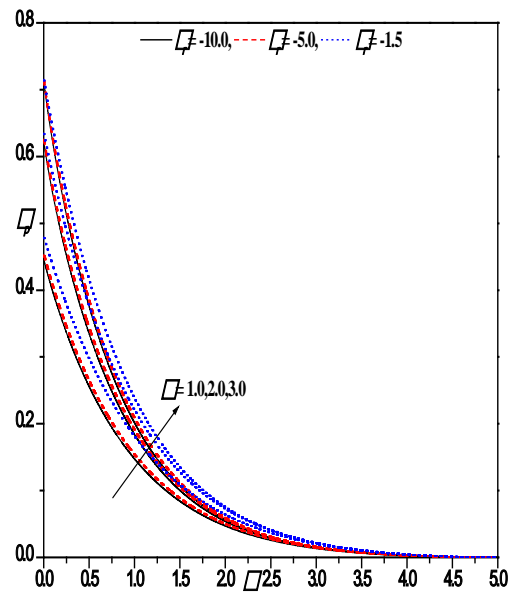


Fig.5(b): Dust phase temperature profiles for different values of K_1 and K_2 with $K_3 = 0.5, K_4 = 0.1, Pr = 1.0$.

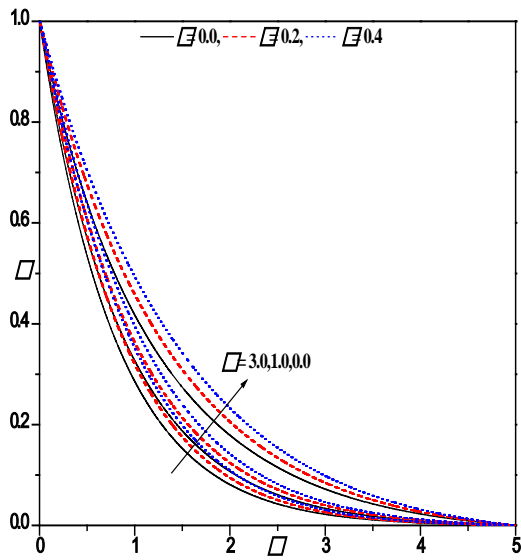


Fig.6(a): Temperature profiles for different values of β and γ with $K_f = 0.5, \Gamma_f = -5.0, Pr = 1.0$.

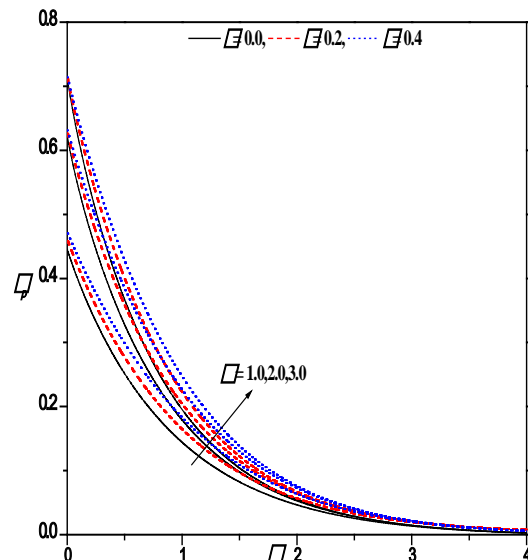


Fig.6(b): Variation of dust phase temperature profiles for different values of β and γ with $K_f = 0.5, \Gamma_f = -5.0, Pr = 1.0$.

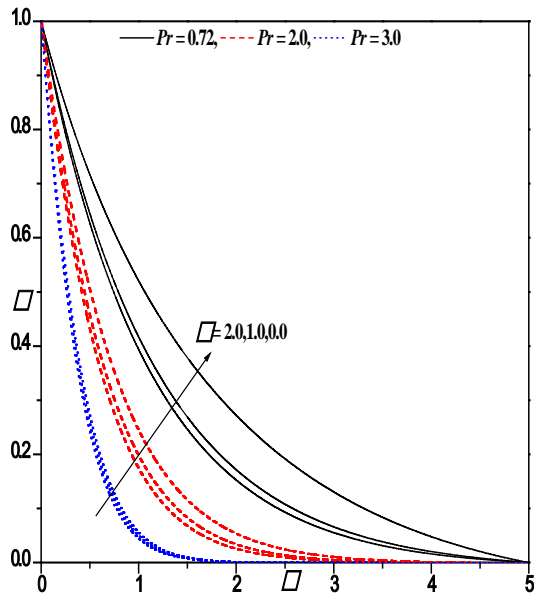


Fig.7(a): Temperature profiles for different values of β and Pr with $K_f = 0.5, \Gamma_f = -5.0, \beta = 0.1$.

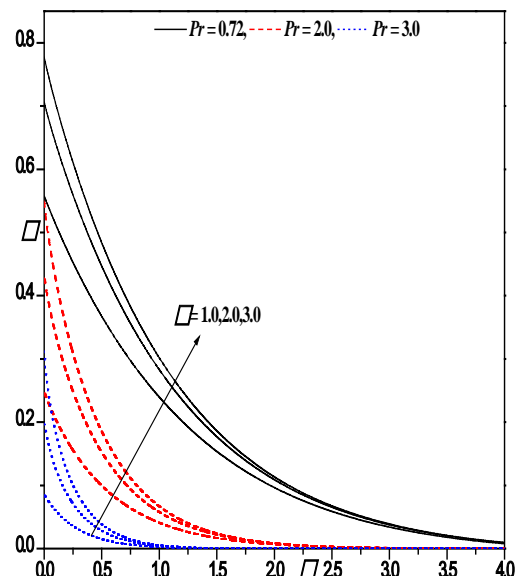


Fig.7(b): Variation of dust phase Temperature profiles for different values of β and Pr with $K_f = 0.5, \Gamma_f = -5.0, \beta = 0.1$.

REFERENCES

- [1].Sakiadis, B.C.: Boundary-layer behavior on continuous solid surface: I. Boundary-layer equations for two-dimensional and axisymmetric flow. *J. AIChE*. Vol.7, p26–28 (1961)
- [2].Sakiadis, B.C.: Boundary-layer behavior on continuous solid surface: II. Boundary-layer equations for two-dimensional and axisymmetric flow. *J. AIChE*.Vol. 7, p221–225 (1961)
- [3].Tsou, F.K., Sparrow, E.M., Goldstain, R.J.: Flow and heat transfer in the boundary layer on a continuous moving surface. *Int. J. Heat Mass Transf.* Vol.10, p219–235 (1967)
- [4].Crane, L.J.: Flow past a stretching plate. *Zeitschrift für Angewandte Mathematik und Physik* **21**, 645 (1970)
- [5].Gupta PS, Gupta TS Heat and mass transfer on a stretching sheet with suction or blowing, *Can J Chem Eng.* (1977) Vol.55:p744–746
- [6].Grubka, L.G., and Bobba, K.M.: Heat transfer characteristics of a continuous stretching surface with variable temperature, *J. Heat Transfer Trans- ASME*, Vol.107, pp. 248–250, 1985.
- [7].Andersson, H.I., Bech, K.H., and Dandapat, B.S., 1992, “Magnetohydrodynamic flow of a power law fluid over a stretching sheet,” *Int. J. Non-Linear Mech*, Vol.27, pp. 929–936.
- [8].Ali, M.E., 1994, “Heat transfer characteristics of a continuous stretching surface,” *Warme-und Stoffubertragung*, Vol.29, pp. 227-234.
- [9].Chen, C.H., 1998, “Laminar mixed convection adjacent to vertical continuously stretching sheets,” *Heat Mass Transfer*, Vol.33, pp. 471-476.
- [10].PS Datti, KV Prasad, M Subhas Abel, A Joshi, MHD visco-elastic fluid flow over a non- isothermal stretching sheet, *Int. J of engineering science*, Vol.42 (8),pp 935-946
- [11].T. Akyildiz, D.A. Siginer, K. Vajravelu, J.R. Cannon and R.A. Van Gorder, Similarity solutions of the boundary layer equations for a nonlinearly stretching sheet, *Math. Methods Appl Sci.* Vol. 33 (2010) 601–606.
- [12].R.A.Van Gorder and Vajravelu, A note on flow geometries and the similarity solutions of the boundary layer equations for a nonlinearly stretching sheet, *Arch. Appl. Mech.* Vol. 80 (2010) 1329–1332.
- [13].Vajravelu .K, Flow and Heat Transfer in a Saturated Porous Medium over a Stretching Surface, *ZAMM – Vol. 74, 12*, pp 605–614, 1994
- [14].D.A.S. Rees, L. Storesletten, The effect of anisotropic permeability on free convective boundary layer flow in porous media, *Transport Porous Media* 19 (1995) 79-92.
- [15].L. Storesletten, D.A.S. Rees, An analytical study of free convective boundary layer flow in porous media: the effect of anisotropic diffusivity, *Transport Porous Media* 27 (1997) 289-304.
- [16].D.A.S. Rees, L. Storesletten, The linear instability of a thermal boundary layer with suction in an anisotropic porous medium, *Fluid Dyn. Res.* 30 (2002) 155-168.
- [17].D.A.S. Rees, L. Storesletten, A.P. Basson, Convective plume paths in anisotropic porous media, *Transport Porous Media* 49 (2002) 9-25.

- [18].Subhas Abel, Sujit Kumar Kha, K.V. Prasad, Study of visco-elastic fluid flow and heat transfer over a stretching sheet with variable viscosity, *Int J of Non-Linear Mechanics*, Vol.37 (2002) pp 81-88.
- [19].Subhas Abel, Ambuja joshi, K.V. Prasad and Mahaboob Ali, Hydromagnetic visco-elastic fluid flow and heat transfer over a non isothermal stretching surface embedded in a porous medium, *I.J.Trans Phenomean*,2002,Vol.4,pp 225-233.
- [20].Subhas Abel, K.V. Prasad and Mahaboob Ali, Convective heat transfer in the flow of visco-elastic fluid stratified in a porous medium over a non-isothermal stretching sheet, *ASME 2003 Int. Mech. Eng. Congress and Exposition*, pp 721-744.
- [21].Pal D, Shivakumara IS Mixed Convection heat transfer from a vertical heated plate embedded in a sparsely packed porous medium. *Int J Appl Mech Eng* (2006) Vol.11(4):929–939.
- [22].T. Hayat, T. Javed, Z. Abbas, Slip flow and heat transfer of a second grade fluid past a stretching sheet through a porous space, 2008, *Int.J. Heat Transfer Trans* Vol 51, pp 4528–4534.
- [23].Chakrabarti, K. M., 1977, “Note on Boundary Layer in a Dusty Gas,” *AIAA Journal*, 12, pp. 1136-1137.
- [24].Datta, N., and Mishra, S. K., 1982, “Boundary layer flow of a dusty fluid over a semi-infinite flat plate,” *Acta Mech*, 42, pp. 71-83.
- [25].Parul Saxena, Manju Agarwal, “Unsteady flow of a dusty fluid between two parallel plates bounded above by porous medium” *International Journal of Engineering, Science and Technology* Vol. 6, No. 1, 2014, pp. 27-33
- [26].T.C. Chiam, Heat transfer with variable thermal conductivity in a stagnation point flow towards a stretching sheet, *Int. Comm. Heat Mass Transfer*. Vol. 23 (1996), 239-248.
- [27].I.A. Hassanien, The effect of variable viscosity on flow and heat transfer on a continuous stretching surface, *ZAMM*. Vol. 77 (1997), 876–880.
- [28].M. Subhas Abel, S.K. Khan and K.V. Prasad, Study of visco-elastic fluid flow and heat transfer over a stretching sheet with variable fluid viscosity, *Int. J. Non- Linear Mech*. Vol. 37 (2002), 81–88.
- [29].K.V. Prasad, K. Vajravelu and P. S. Datti, The effects of variable fluid properties on the hydromagnetic flow and heat transfer over a non-linearly stretching sheet, *Int. J. Ther. Sci*. Vol. 49 (2010), 603-610.
- [30].T. Cebeci and P. Bradshaw, *Physical and Computational Aspects of Convective Heat Transfer*, Springer-Verlag, New York (1984).
- [31].H.B. Keller, *Numerical Methods for Two-point Boundary Value Problems*, Dover Publ., New York (1992).
- [32].K. Vajravelu and K.V. Prasad, *Keller-box method and its application*, HEP and Walter De Gruyter GmbH, Berlin/Boston (2014).
- [33].Vajravelu, K., and Nayfeh, J., 1992, “Hydromagnetic Flow of a Dusty Fluid Over a Stretching Sheet,” *Int. J. Nonlinear Mech.*, 27, pp. 937–945.